

# Preliminary studies on empirical roll angle error reduction and tidal detection for the Japanese altimetry mission



O. Isoguchi<sup>1</sup>, A. Uematsu<sup>2</sup>, Y. Nakajima<sup>2</sup>, R. Nakamura<sup>2</sup>, Y. Yajima<sup>2</sup>, M. Ohki<sup>2</sup>, and A. Shinozaki<sup>1</sup>

1.Remote Sensing Technology Center of Japan 2.Japan Aerospace Exploration Agency

## Introduction

Japan Aerospace Exploration Agency (JAXA) is working on a conceptual study of altimeter mission named Coastal and Ocean measurement Mission with Precise and Innovative Radar Altimeter (COMPIRA), which will carry a wide-swath altimeter named Synthetic aperture radar (SAR) Height Imaging Oceanic Sensor with Advanced Interferometry (SHIOSAI).

As preliminary studies on sea level anomaly (SLA) measurements by COMPIRA, we conducted simulations about 1) the reduction of roll angle errors which is peculiar to the SAR-typed altimeter and 2) the effect of the wide-swath SSH observation on tide detection in the marginal and coastal seas where the tide model derived by traditional nadir-type altimeters is not accurate enough to derive SLAs.

## Empirical roll error estimation

Following the previous studies (i.e., Dibarboure et al., 2011), the crossover method was conducted to examine the effect of the proposed COMPIRA orbit configuration (Table 1) on the roll angle error reduction. Fig.1 shows observation times per cycle by COMPIRA, representing about 1.8 times observation around Japan.

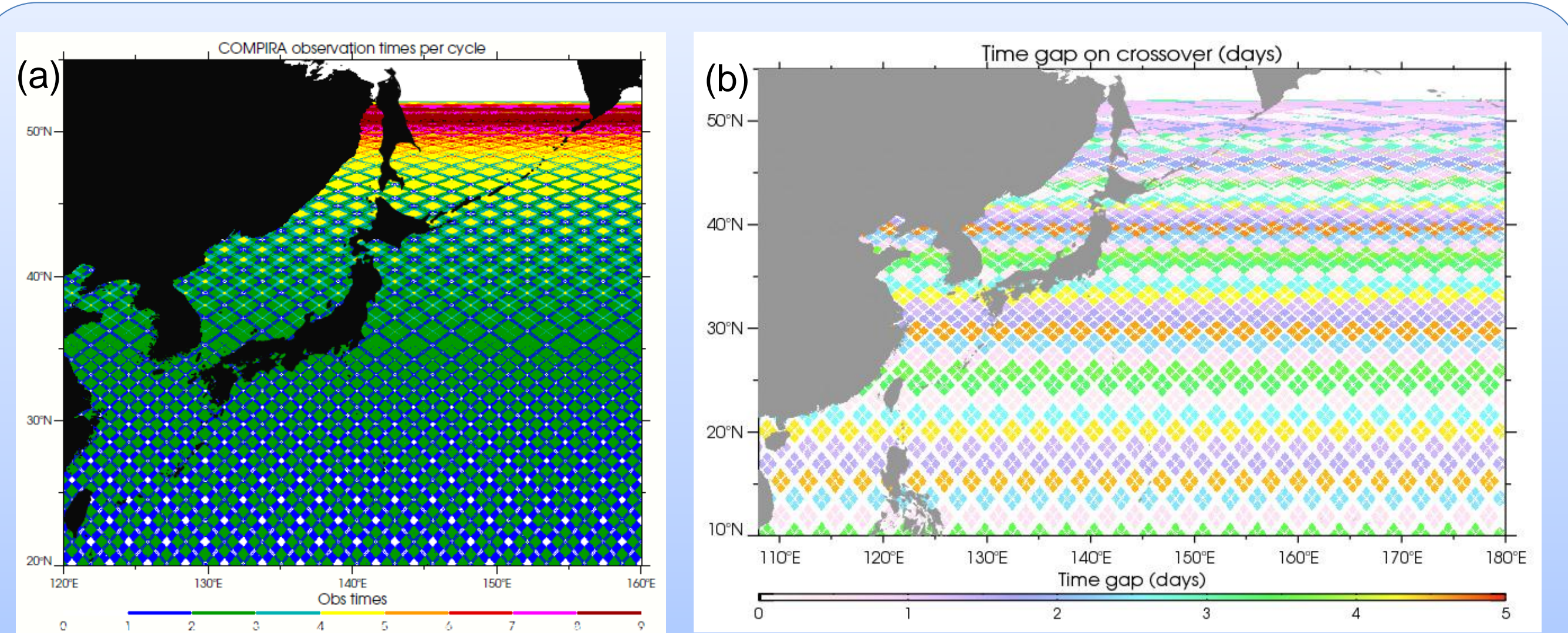


Fig. 1. (a) Observation times per cycle by COMPIRA, and (b) temporal gap between ascending and descending observations on crossover areas.

Table 1. COMPIRA orbit configuration.

Parameters	Revisit time	Inclination	altitude	swath
	9.8671 days	51 deg.	937 km	80km × 2

## Basic simulation

### 1. Simulated SSH (Hreal)

Model SSHs are virtually observed with COMPIRA orbits for a year to simulate SSH (Hreal). Ocean model used is JCOPE (Japan Coastal Ocean Predictability Experiment) 2 which was provided by JAMSTEC.

### 2. Adding errors

Table 2 represents error added to the model SSH (Hreal).

Table 2. Characteristics of errors to be added to the model SSH.

Error factors	case1			case2		
	Amplitude	Along-track period	Cross-track period	Amplitude	Along-track period	Cross-track period
Roll angle	0.3 arcsec	22200km	linear	1 arcsec	800km	linear
Base line length	5000km	quadratic		5000km	quadratic	
orbit	2cm	5000km	constant	2cm	5000km	constant
Sensor (5km×5km)	5cm	Random	random	5cm	Random	random
Wet tropospheric delay	5cm	50km	50km	5cm	50km	50km

### 3. Local estimation and evaluation

Roll angles are estimated at each crossover from SSH difference ( $\Delta$ Hobs) and cross-track distances by a least square method. Estimated angles are then evaluated comparing with the given angles. Fig. 2 show RMS error maps of estimated roll angles for the case 1 and case 2 simulations, which indicate large errors in the Kuroshio Extension and relatively large temporal gap crossovers (see, Fig.1(b)).

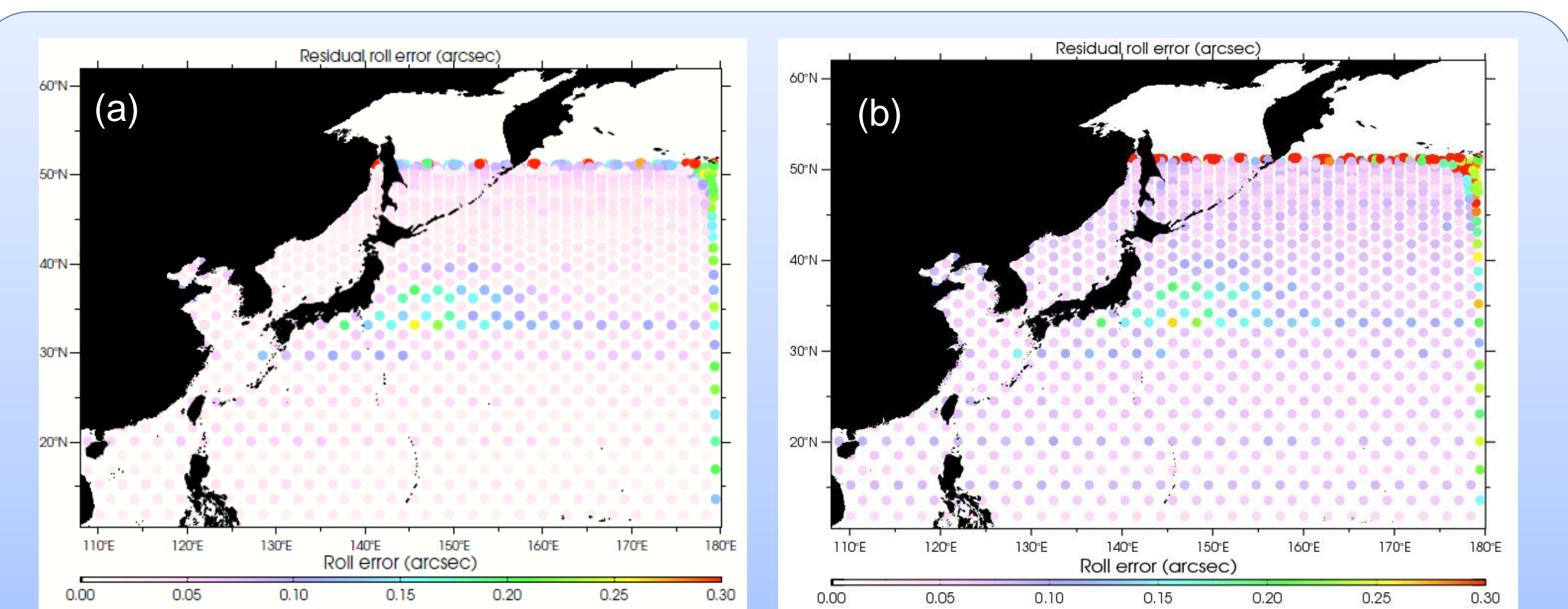


Fig. 2. RMS error maps of residual roll angles for (a) the case 1 and (b) case 2 simulations.

Table 3. Mean RMS errors of estimated roll angles for the cases 1 and 2.

	Case 1		Case 2	
Mean RMS errors	0.051(arcsec)	2.0cm@ 80km	0.075(arcsec)	2.9cm @ 80km

## Sensitivity experiments

In order to examine the effect of period of roll angle error, sensitivity experiments are conducted by changing the along-track error period of Case1 following Table 4. The resultant RMS maps and mean values of residual roll angles are shown in Table 4 and Fig. 3, which indicates that residual roll angle errors are not reduced for the cases 3 to 6 which roll angle error periods are shorter than 60s.

Table 4. Defined roll angle error periods.

	Case3	Case4	Case5	Case6	Case7	Case8
Along-track period	31km (5s)	62km (10s)	123km (20s)	184km (30s)	370km (60s)	738km (120s)
Residual RMS errors (arcsec)	0.217 (8.4cm)	0.2164 (8.4cm)	0.2635 (10.2cm)	0.2229 (8.6cm)	0.0997 (3.9cm)	0.0573 (2.2cm)

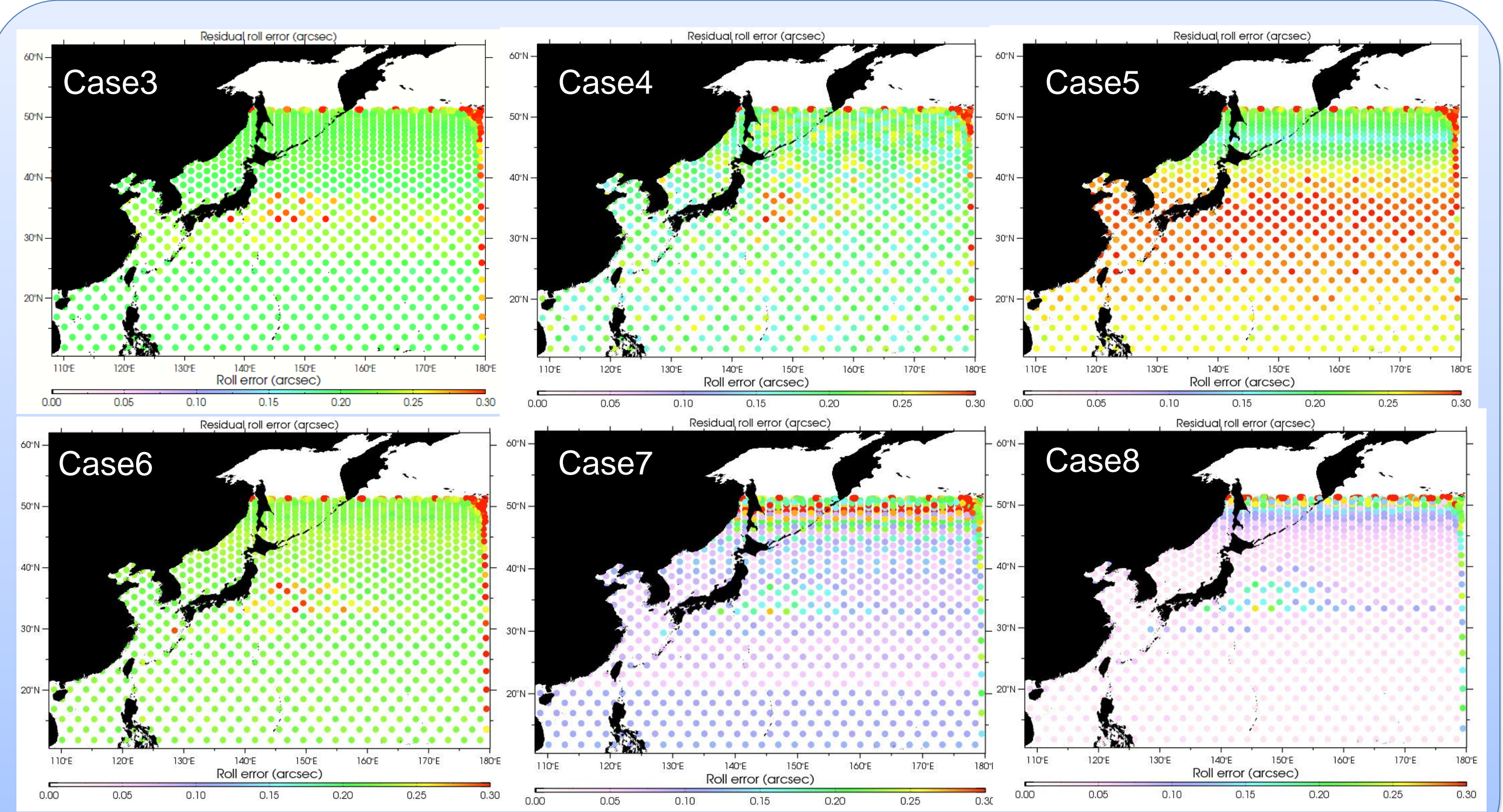


Fig. 3. RMS error maps of residual roll angles for the case 3 to 8 simulations.

## Effect of wide-swath measurements on tide detection

One of the promising advantage of wide-swath SSH measurements is improving a tide model in marginal seas. Especially since East China Sea and Yellow Sea are one of the most energetic regions, the current tide model there is not good enough to detect the current-related SSH. The effect of wide-swath SSH measurements on the tide detection in the marginal seas around Japan is evaluated in a very simple way.

### 1. Simulated tide SSHs

Tide model outputs are virtually observed with COMPIRA orbits for three years. The tide model used is NAO.99b (Matsumoto et al., 2000).

### 2. Harmonic analysis

Harmonic analysis using major 8 constituents, Sa, Ssa, Mu, and MM is performed for the time series of simulated SSHs.

### 3. Spatial interpolation

Calculated amplitudes and phases are interpolated into  $0.25 \times 0.25^\circ$  grid, where  $0.25\text{deg}$  and  $1.0\text{deg}$  e-folding scales are applied for wide-swath and nadir results.

### 4. Evaluation

RMS errors between tide model SSHs and those reconstructed from the derived amplitudes and phases are calculated (Fig.4 and Table.5).

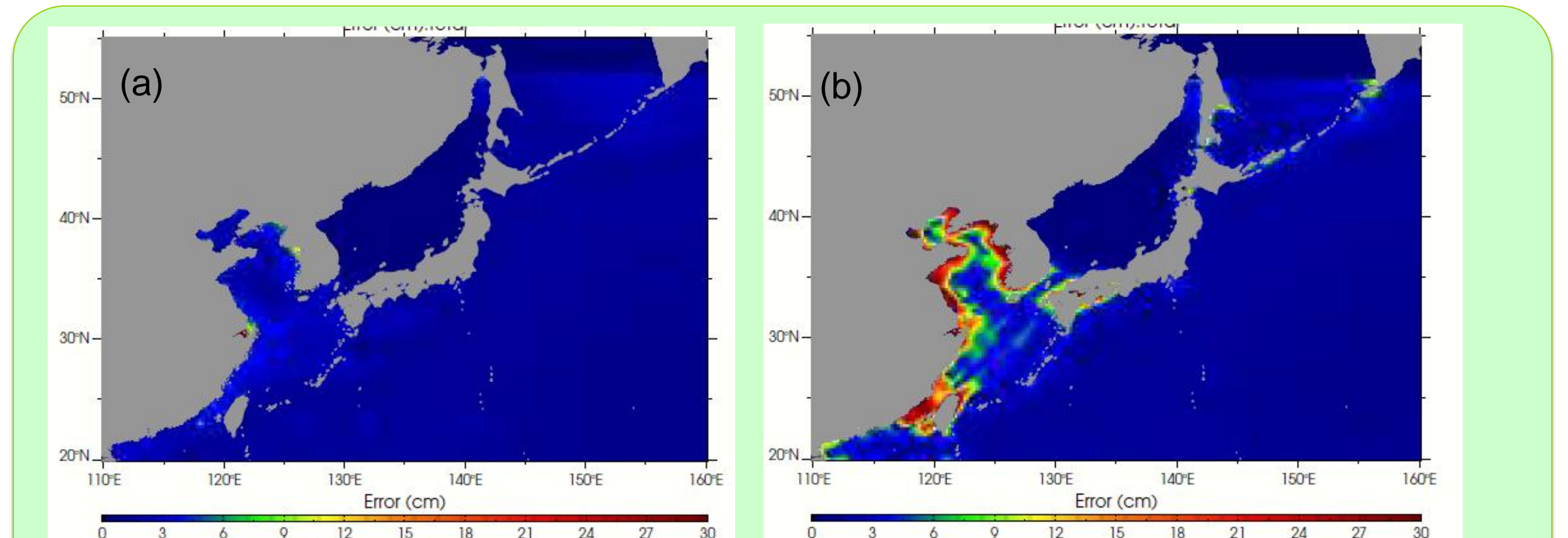


Fig. 3. RMS error maps of tide SSHs of major 8 constituents detected by COMPIRA (a) wide-swath and (b) nadir only observations.

Table 5. RMS errors (in cm) for major 8 constituents in East China Sea and Yellow Sea.

	M2	S2	N2	K2	K1	O1	P1	Q1	total
COMPIRA	1.06	0.48	1.01	0.71	0.82	0.78	1.05	0.41	2.59
Nadir	8.28	3.44	2.01	1.45	1.58	1.35	0.97	0.41	9.87

## Future plans

- ✓ Temporal interpolation and global evaluation should be included.
- ✓ Base line error estimation and their sensitivity tests are also required.
- ✓ Co-linear and direct (using DEM) methods will be tested and combined with the crossover results.